coatings

MDPI

Article

Diffusion Effect on Octogen Coating-Curing Kinetics with Polyurethane Using Infrared Spectroscopy

Heri Budi Wibowo [1,*], Hamonangan Rekso Diputro Sitompul [1], Yudha Budiman [1], Bagus Wicaksono [1], Ahmad Jamaludin Fitroh [1], Ahmad Riyadl [1], Wiwiek Utami Dewi [1], Yulia Azatil Ismah [1], Dwi Setyaningsih [1], Aprilia Fitri Yastuti [1], Mohamad Baiquni [2], Lilis Mariani [1], Anggaria Maharani [3], Herry Purnomo [1], Kendra Hartaya [1], Retno Ardianingsih [1], Luthfia Hajar Abdillah [1] and Sutrisno Sutrisno [1]

[1] Aeronautics and Space Research Organization, National Research and Innovation Agency, Cibinong 16911, West Java, Indonesia; hamo001@brin.go.id (H.R.D.S.); yudh002@brin.go.id (Y.B.); bagu005@brin.go.id (B.W.); ahma056@brin.go.id (A.J.F.); ahma052@brin.go.id (A.R.); wiwi015@brin.go.id (W.U.D.); yuli042@brin.go.id (Y.A.I.); dwis011@brin.go.id (D.S.); apri012@brin.go.id (A.F.Y.); lili007@brin.go.id (L.M.); herr010@brin.go.id (H.P.); kend001@brin.go.id (K.H.); retn014@brin.go.id (R.A.); luth002@brin.go.id (L.H.A.); sutr004@brin.go.id (S.S.)

[2] Directorate of Laboratory Management, Research Facilities, and Science and Technology Area, Research and Innovation Infrastructure, National Research and Innovation Agency, Central Jakarta 10340, Jakarta, Indonesia; moha040@brin.go.id

[3] Energetic Material Center, DAHANA Co., Subang 41285, West Java, Indonesia; angaria.maharani@dahana.id

* Correspondence: heribw@gmail.com; Tel.: +62-021-4892802

Abstract: The kinetic analysis of octogen coating with a polyurethane base containing hydroxyl-terminated polybutadiene (HTPB) was investigated using infrared spectroscopy. The coating process involved a solvent method, where octogen and liquid polyurethane were mixed, the solvent was evaporated, and curing took place at an elevated temperature. The ratio of HTPB to diisocyanate was equimolar. About 200 g octogen was coated with mixture of 2 mL HTPB, 50 mL ethyl acetate, and 0.2 mL TDI in the glass beaker at 30 °C for 1 h. The filtrated ethyl acetate was then evaporated, and the residue was dried in a vacuum oven for 15 min at 30 °C. The resulting film-coated octogen was cast into a KBr pellet and cured in the oven for 7 days at 40 °C, then infrared-analyzed every hour during the curing process. After curing, the shape of the coated octogen particles was analyzed using SEM Initially, the curing process occurred in the solvent system, followed by further curing in the bulk system. The kinetic analysis was performed using a modified diffusion-autocatalytic model, which includes noncatalytic, autocatalytic, and diffusion components. This model was compared with others during the bulk reaction and proved to be effective in correcting errors, particularly in the gel time region. Thermodynamic parameters were evaluated using the Arrhenius and Eyring equations. The reaction rate was initially controlled by chemical reactivity, but after the gel time, diffusion became the controlling factor. In the HTPB-TDI system, both the noncatalytic and autocatalytic parts decreased with increasing temperature, while diffusivity increased. It is worth noting that diffusivity is temperature-dependent. Different di-isocyanates, namely toluene diisocyanate (TDI), iso-phorone diisocyanate (IPDI), and hexamethylene diisocyanate (HMDI), were studied, revealing that HMDI exhibited higher reactivity than TDI and IPDI. The catalyst effect on reaction rate of the HTPB-TDI system was investigated. The addition of catalysts (0.1%) to the HTPB-TDI system decreased their activation energy in the order DBTL > FeAA > TPB. Catalysts did not change their diffusivity.

Keywords: polyurethane coating; kinetic; octogen; coating; curing; HTPB

check for updates

Citation: Wibowo, H.B.; Sitompul, H.R.D.; Budiman, Y.; Wicaksono, B.; Fitroh, A.J.; Riyadl, A.; Dewi, W.U.; Ismah, Y.A.; Setyaningsih, D.; Yastuti, A.F.; et al. Diffusion Effect on Octogen Coating-Curing Kinetics with Polyurethane Using Infrared Spectroscopy. *Coatings* **2023**, *13*, 1584. https://doi.org/10.3390/coatings13091584

Academic Editor: Fengwei (David) Xie

Received: 31 July 2023
Revised: 28 August 2023
Accepted: 30 August 2023
Published: 11 September 2023

Copyright: © 2023 by the authors. Licensee MDPI, Basel, Switzerland. This article is an open access article distributed under the terms and conditions of the Creative Commons Attribution (CC BY) license (https://creativecommons.org/licenses/by/4.0/).

1. Introduction

Hexogen and octogen are both highly explosive materials. They are used as oxidants in homogeneous propellants due to their high energy content, substituting ammonium perchlorate in composite propellant formulations (APCP) [1–3]. The addition of coated

hexogen to the composite propellant formulation can increase its energetic properties and reduce smoke emissions. However, these explosives have disadvantages, as they are sensitive and not compatible with the HTPB (hydroxyl-terminated polybutadiene) binder, necessitating a coating process [3–11].

Hexogen powder has been successfully coated using polyurethane-based HTPB through a solvent method. In this process, the powder is mixed with the coating solution, and polymerization is initiated within the solution. Subsequently, the solvent is evaporated, and the polyurethane coating is cured at an elevated temperature. There is limited research information about explosive coating kinetics; most publications have focused on characterizing the coated hexogen and their propellant properties.

Additional research is needed to further investigate and understand the coating kinetics of octogen with polyurethane-based HTPB, as well as the potential for using different catalysts and di-isocyanates in the coating process. Catalysts play a significant role in accelerating the reaction rate during polymerization. Some suitable catalysts for polyurethane include tri-ethylene diamine (TEDA), dibutyl tin laurate (DBTL), tin (II) 2-ethyl hexanoate, and tris phosphine bismuth (TPB). Additionally, there are several di-isocyanates that can be used as curing agents, such as toluene diisocyanate (TDI), isophorone diisocyanate (IPDI), phenyl diisocyanate (PDI), and hexamethylene diisocyanate (HMDI). This paper focuses on the kinetic approach of coating octogen with polyurethane-based HTPB using varied di-isocyanates (TDI, IPDI, and HMDI) and the most commonly used catalysts (TPB, FeAA, and DBTL) [3,5,7,12].

Polyurethane curing kinetics has been extensively studied using various methods such as infrared spectroscopy, NMR, viscosity, and heat release measurements [12–16]. Among these, infrared spectroscopy stands out as the simplest, most accurate, rapid, and cost-effective method for evaluating this kinetic model. The reaction conversion is assessed by observing the absorption of isocyanate groups, with polybutadiene methyl groups used as an absorption reference. Quantitative analysis is then performed using a calibration curve. The coating and infrared characterization of hexogen are successfully achieved using polyurethane and Viton [1,2].

The kinetics of bulk polyurethane formation has been investigated intensively. The noncatalytic model is based on the formation of linear polyurethane between alcohol (HTPB) and diisocyanate. This model is suitable for conditions with low viscosities up to just before gel time. The autocatalytic model includes a crosslinking reaction between the urethane and excess diisocyanate. This model is suitable for slurries with high viscosity; however, there are many deviations in the polyurethane curing process at higher temperatures and very high viscosity. Under these conditions, the influence of mass diffusivity is assumed to occur alongside polymerization and crosslinking reactions. To address this, the modified autocatalytic model was developed, taking diffusion effects into account.

In the powder coating process using the solvent method, the curing occurs through two reaction stages. Initially, the curing reaction is initiated in the solution phase during the mixing of HTPB, diisocyanate, and substrate. At this stage, the reactant molecules exhibit high activity, allowing for easy migration and collision, and the reaction is primarily controlled by their chemical reactivity. As the reaction progresses, after the gel time, the second stage of curing takes place in a solid coating film formed when all solvents evaporate [1,3–8]. During this stage, the activity of the reactant molecules is hindered by their diffusivity in the film. The reactivity of system isopropyl diol and phenyl diisocyanate is controlled by their diffusivity in the film state at high temperature and high viscosity [8].

In the initial stage, the reactants display high activity, and the reaction is mainly governed by their chemical reactivity. However, after the evaporation of solvents, the reaction rate is then controlled by film diffusion. For the coating system involving isopropyl di-alcohol and methylene diisocyanate, the first curing stage is governed by chemical reactivity, while the subsequent curing stage is controlled by intrafilm diffusion at higher temperatures [17]. Therefore, investigating the diffusivity effect on the kinetic process during the coating is essential.

The kinetics of octogen coating with polyurethane-based HTPB is studied using infrared spectroscopy with varied di-isocyanates and catalysts. The diffusion effect on the reaction rate and thermodynamic parameters, such as activation energy, enthalpy, and entropy, is studied using the modified autocatalytic model. Additionally, the temperature effect on the reaction is determined using the Arrhenius and Eyring equations.

2. Materials and Methods

2.1. Materials

Octogen was supplied by DAHANA, Co., Ltd., Subang, Indonesia. Ethyl acetate for pure analysis was supplied by Merck, Jakarta, Indonesia. HTPB, IPDI, TDI, HMDI, DBTL, TPB, and FeAA (ferric acetylacetonate) were supplied by Dalian, Co., Ltd., Dalian, China. The HTPB (hydroxyl-terminated polybutadiene) has a hydroxyl number of 40, functionality of 1.9, average molecular weight of 3000 g/mol, and dispersity of 1.3. The particle size of the octogen was 100 microns.

2.2. Instrumentations

Infrared qualitative and quantitative analysis was conducted using a Hitachi (Tokyo, Japan) IR-Prestige Serial A210043 infrared spectrometer with a standard liquid cuvette, covering the wavelength range of 400–4000 cm^{-1} [9–11]. The coating depth was measured using a scanning electron microscope (SEM) Phenom Word Pro X Desktop (Thermo Fisher Scientific, Waltham, MA, USA) [8,9,13]. The particle size of the octogen was measured with a particle size analyzer PSA-CILAS 1190 Liquid (Orleans, France).

2.3. Procedure

A mixture of 4 mL of HTPB, 50 mL of ethyl acetate, 0.4 mL of TDI, and 200 g of octogen is prepared in a 500 mL glass beaker and stirred for 60 min [12,14]. The molar ratio of isocyanate to hydroxyl was maintained as equimolar (R = 1). Approximately 1 mL of the mixture is withdrawn as a sample every 5 min, dissolved in 100 mL of benzene, and analyzed using infrared spectroscopy [18–20]. The filtrated ethyl acetate is then evaporated, and the residue is dried in a vacuum oven for 15 min at 30 °C. The resulting film-coated octogen is cast into a KBr pellet and cured in the oven for 7 days at 40 °C. The cured and coated octogen is subjected to infrared analysis every 1 (one) hour during the curing process. After curing, the shape of the coated octogen particles is analyzed using SEM [21,22]. This procedure is repeated for vacuum oven temperature 40, 50, 60, 70 °C.

The above procedure is repeated using different di-isocyanates, namely IPDI and HMI. Additionally, the effect of catalysts is studied by adding 0.1 g of FeAA, DBTL, and TPB as catalysts.

2.4. Analysis

The conversion of reacted isocyanate concentration is determined by measuring the change in isocyanate concentration, which is identified through infrared absorption of the isocyanate stretching vibration in the isocyanate group, occurring at 2250–2275 cm^{-1}. To establish a constant reference, the absorption of CH_3 vibration in the polybutadiene (HTPB) at 2850–2950 cm^{-1} is used, where this absorbance is constant. The reaction conversion of isocyanate (α) is calculated using Equation (1) based on Beer's law, where A^o_{NCO} and $A^o_{CH_3}$ represent the initial absorbance of NCO and CH_3 absorption, respectively [7,23].

$$\propto = 1 - \frac{A_{NCO}/A_{CH_3}}{A^o_{NCO}/A^o_{CH_3}} \quad (1)$$

2.5. Kinetics Model

The kinetic model for polyurethane formation from HTPB and diisocyanate is based on the reaction of hydroxyl groups from HTPB with isocyanate from diisocyanate, resulting in the production of urethane groups, as shown in Equation (2). The mechanism of this

reaction is complex [7,18,19,23]. The polymerization process involves the addition of chains of urethane. The kinetic model based on the reaction of functional groups showing a reaction of n-order, as expressed in Equation (3), where α, k, and n are conversion, rate constant, and reaction order. This model is referred to as the noncatalytic model and effectively predicts the formation of polyurethane at low polymer chain lengths or before the gel time.

$$\text{-N=C=O + HO-} \rightarrow \text{-NH-CO-O-} \quad (2)$$

$$\frac{d \propto}{dt} = k(1- \propto)^n \quad (3)$$

The noncatalytic model struggles to accurately predict the reaction rate profile for higher polymer chains after the gel phase. To address this limitation, the model incorporates an autocatalytic reaction between urethane and isocyanate, leading to the production of crosslink allophanate as described in Equation (4). This autocatalytic reaction becomes more prominent at higher temperatures when there is an excess of isocyanate in present in composition. The model incorporates two reaction rates constants: k_1 for linear polymerization contribution and k_2 for crosslink contribution, expressed in Equation (5). The crosslink reaction follows an m-order reaction.

$$\text{-N=C=O + -NH-CO-O-} \rightarrow \text{-N-(CO-O-)(CO-NH-)} \quad (4)$$

$$\frac{d \propto}{dt} = (k_1 + k_2 \propto^m)(1- \propto)^n \quad (5)$$

This polyurethane formation is well predicted, but deviations increase at higher temperatures. The model is controlled by chemical reaction kinetics, and the diffusion is negligible. The diffusion's contribution to polyurethane curing is proposed to be related to the crosslink reaction and is expressed in Equation (6), where D represents diffusivity. D and m are affected by the reaction temperature. Based on Fick's law for non-Newtonian fluid, liquid diffusivity depends on their temperature, pressure, and composition [22]. The diffusion part contribution is expressed by (D/(D + α)) or 1/(1 + α/D), where D is the diffusivity constant. The value of (D/(D + α)) is changed with conversion, but the D value is constant.

$$\frac{d \propto}{dt} = k_1(1- \propto)^n + \frac{k_2 \propto^m (1- \propto)^n}{1 + (\propto/D)} \quad (6)$$

The thermodynamic parameters are evaluated using the Arrhenius and Eyring relations, which are expressed in Equations (7) and (8) [13,22,24]. In these equations, the symbols k, E, A, ΔS, and ΔH represent the reaction rate constant, activation energy, collision frequency, enthalpy, and entropy of the i-th reaction. Additionally, R, T, h, and N represent the ideal gas constant (8.314 $J \cdot mol^{-1} \cdot K^{-1}$), reaction temperature (K), Planck constant (6.626×10^{-34} J·s), and Avogadro number (6.022×10^{23} mol^{-1}).

$$ln\ k_i = -\frac{E_i}{RT} + \ln A_i \quad (7)$$

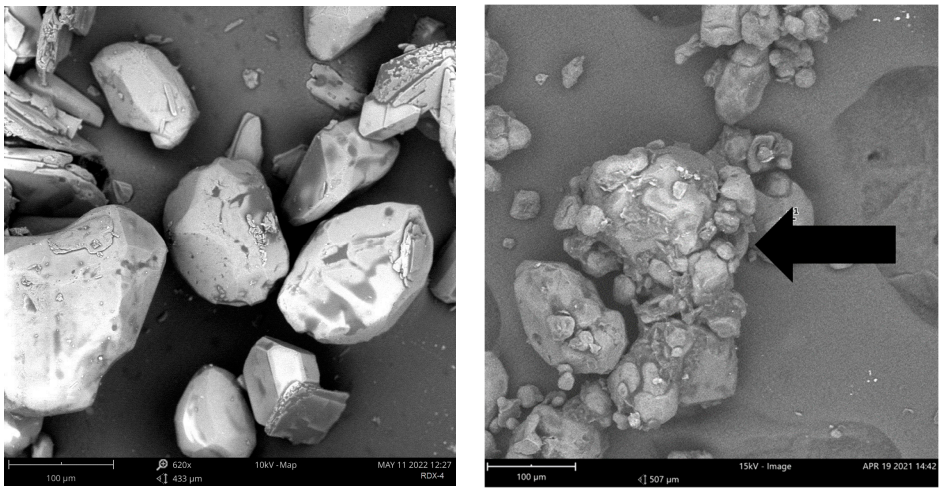
$$\ln(k_i/T) = -\frac{\Delta H_i}{RT} + \frac{\Delta S_i}{R} + \ln \frac{R}{Nh} \quad (8)$$

3. Results and Discussion

3.1. Coating Identification

The particle size analysis revealed a significant increase in the size of octogen particles, from 100 to 200 microns. Figure 1 shows the SEM image of the initial octogen (a) and coated octogen particles (b). The circularity and roundness of the particles were calculated using Image-J software (https://imagej.net/), and it was observed that the coating of octogen increased their circularity from 0.74 to 0.76, while the roundness has increased

from 0.67 to 0.72. The presence of mounds, as indicated by arrows, signified the presence of a polyurethane layer coating on the octogen particles. Based on the image and particle size analysis, it could be concluded that octogen had been well-coated with polyurethane-based HTPB. These results aligned with the earlier researchers who studied the coating of hexogen with HTPB-based polyurethane [7,18,25,26].



(**a**) (**b**)

Figure 1. SEM analysis of octogen (**a**) and coated octogen (**b**) with polyurethane HTPB-TDI.

3.2. IR Identification

Figure 2 displays the infrared spectra of coated octogen in both the slurry (a) and film state (b). The octogen was identified by its characteristic absorption bands, including nitro groups at 1566 cm^{-1} (νs NO_2), 1142 cm^{-1} (ν ring), 964 and 949 cm^{-1} (stretching bands), 833 and 764 cm^{-1} (δ and γ NO_2), and 625 and 602 cm^{-1} (T + γ NO_2) [1,2,7,18]. These characteristic absorption bands were also observed in the spectra of coated octogen.

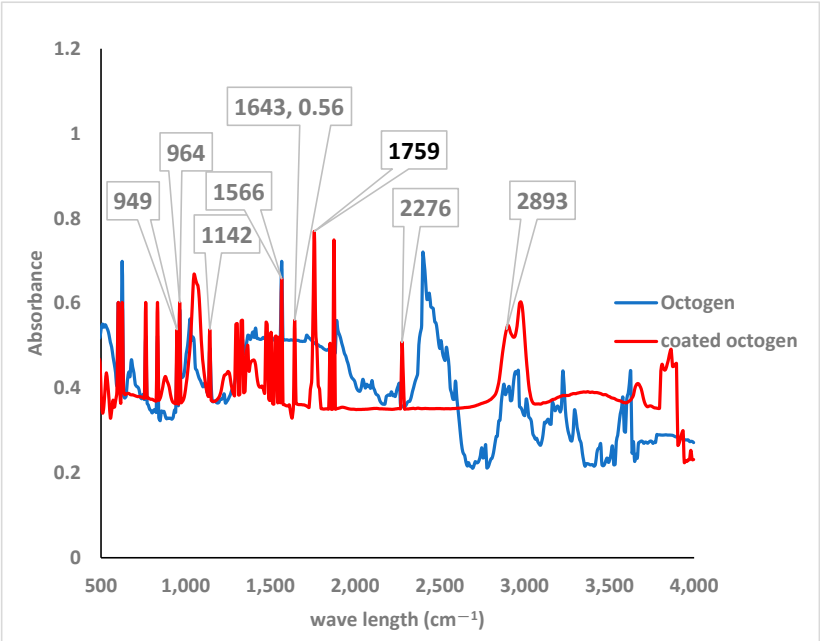
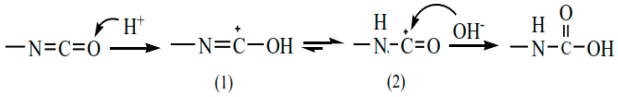


Figure 2. The infrared spectra of coated octogen using polyurethane HTPB-TDI.

The polyurethane was produced through a reaction between isocyanate and alcohol [3]. The isocyanate group induced the formation of electrophilic centers at nitrogen atoms and

nucleophilic centers at oxygen atoms. Nucleophiles containing active hydrogen from HTPB could attack the isocyanate, resulting in the acceptance of hydrogen atoms by oxygen atoms to produce unstable carbonyl groups. After molecular rearrangement, the urethane NCOO groups were formed. This reaction could be identified by a decrease in the isocyanate group's absorption at wavelengths of 2260–2275 cm^{-1}. The polyurethane formation was indicated by an increase in the absorption of C=O stretching at 1600–1750 cm^{-1} and NH stretching at 1500–1550 cm^{-1} [21,27].



(9)

The backbone of HTPB was identified by the absorption of CH_2 stretching and CH_3 at 1640 and 2850–2950 cm^{-1}, respectively. This absorption remained unchanged throughout the reaction. The decrease in isocyanate concentration was identified by the reduction of NCO absorption at 2270 cm^{-1} [1]. At the end of the reaction, there was no absorption of NCO at 2270 cm^{-1}, indicating that all of the isocyanate had reacted. HTPB was further identified by the absorption of C=C stretching and CH_3 stretching at 1640 and 2850–2950 cm^{-1}, respectively. This absorption remained unchanged throughout the reaction, making it suitable as a reference. The formation of polyurethane could be identified by the absorption of C=O stretching vibration at 1710–1760 cm^{-1}.

3.3. Kinetic Evaluation

The modified diffusion–autocatalytic model was applied to the HTPB-TDI system using Equation (6). The logarithmic of Equation (6) is shown in Equation (10). The experimental data were fitted to plot log(dα/dt) versus (1 − α) in Figure 3. The values of 'n' were determined from their intercept, the value of 'm' was calculated from m + n = 2. The value of k_1, k_2, and D were numerical calculated using nonlinear Runge–Kutta estimation. The parameters k_1, k_2, and D were repeated at temperatures 40, 50, 60, and 70 °C, and the kinetic parameter values are summarized in Table 1.

$$\log\left(\frac{d\propto}{dt}\right) = n{\cdot}log(1-\propto) + log\left(k_1 + \frac{k_2 \propto^m}{1+(\propto/D)}\right) \quad (10)$$

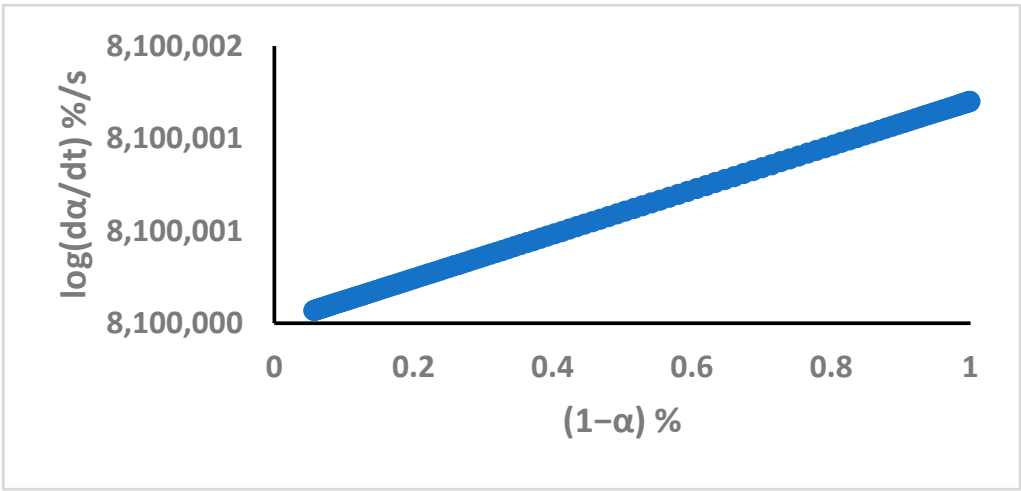


Figure 3. Plot log(dα/dt) versus (1 − α) of HTPB-TDI system.

Table 1. The calculated k_1, m, k_2 and D of HTPB-TDI system at variated temperature.

Temperature (°C)	k_1 (s^{-1})	n	k_2 (s^{-1})	D ($cm^2 \cdot s^{-1}$)	m
30	8.10×10^5	1.2	1.01×10^4	1.51	0.8
40	14.10×10^5	1.2	1.43×10^4	0.41	0.8
50	21.10×10^5	1.2	1.71×10^4	0.31	0.8
60	26.10×10^5	1.2	2.01×10^4	0.23	0.8
70	31.10×10^5	1.2	2.57×10^4	0.11	0.8

The calculated kinetic parameters were compared to the noncatalytic model (Equation (2)) and the autocatalytic model equation (Equation (4)). The fit of calculated cure conversion to the experimental data of the varied model is shown in Figure 4. The modified diffusion–autocatalytic model exhibited a lower error (calculated error = 0.09%) compared to the other models (0.11% and 0.12%). Noncatalytic models tended to yield higher estimates of experimental results than autocatalytic models. The autocatalytic model incorporated an allophane formation reaction as shown in Equation (3). Crosslinks began to appear when a considerable amount of urethane group was formed, primarily near the gel time [28]. A competitive reaction occurred between urethane and allophanate formation, leading to different reaction rates in the gel time regions. The role of diffusivity became evident from the beginning of the gel time to the end of the reaction. The autocatalytic model was improved by adding a diffusion component, which brought the calculated curing conversion closer to the experimental results. Similar results were observed when applying the diffusion model to HTPB-IPDI with high solid content [29]. These results also applied to cases without filler and low concentration, where the diffusion effect significantly corrected the error across the entire reaction range. The influences of chemical reactivity (electronegativity and steric hindrance), crosslink reactions (allophanate formation), and molecule diffusivity had been incorporated into the noncatalytic, autocatalytic, and diffusion parts, respectively.

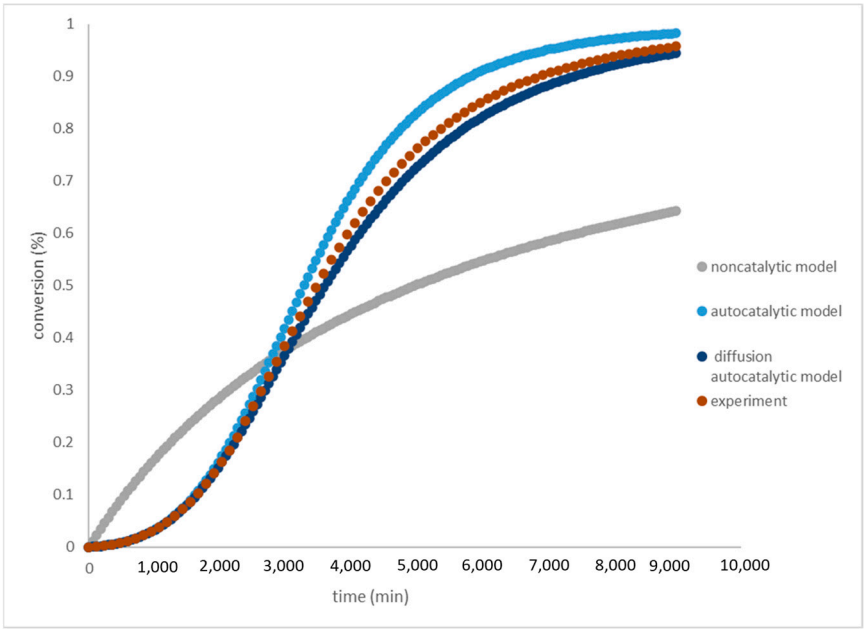


Figure 4. Plotting curing conversion of HTPB-TDI system at variated model.

The reaction initially occurs in solution with low viscosity, where the movement of molecules was not affected by diffusion [29]. The reaction initially occurred in solution with

low viscosity, where the movement of molecules was not affected by diffusion [29]. This was because the reaction was carried out without solvents or at high concentrations, allowing diffusivity to take effect at the beginning of the reaction. As the gel time approached, the profile started to deviate lower than the experimental data because some urethane groups reacted with the isocyanate to form allophanate. Both the autocatalytic part and diffusivity significantly contributed to the curing conversion, and all parts significantly contributed to the reaction rate. After the gel time, the diffusivity part became dominant in contributing to the reaction rate, as seen by the increasing total rate constant every ten degrees temperature. With every ten-degree increased in temperature, the total constant rate increases by 1.1 (less than 1.2), indicating that diffusion controls the reaction rate.

The catalytic rate constant (k_1) decrease is sharper than the catalytic rate constant (k_2), which is shown in the slope of Figure 5. This phenomenon was commonly observed in polyurethane systems, similar to HTPB-IPDI [29]. Based on the reaction mechanisms described in Equations (1) and (3), the isocyanate group was more susceptible to attack by nucleophilic H^+ from hydroxylated HTPB than from urethane [30]. This observation was supported by infrared spectrometer results, which consistently shown the presence of the urethane group (indicated by C=O stretching vibration absorption) along with the appearance of the allophanate group.

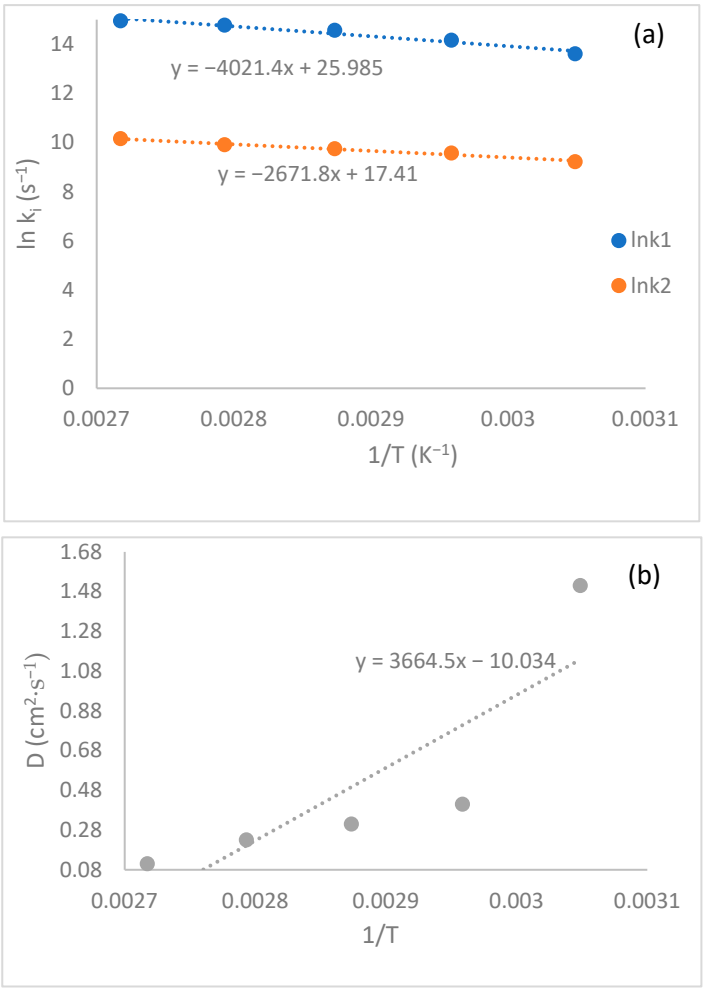


Figure 5. Plotting ln k vs. 1/T (**a**) and D versus 1/T (**b**) HTPB-TDI system.

The temperature-raising effect in Figure 5 showed that both k_1 and k_2 increased, while D decreased. This phenomenon aligned with the behavior observed in the diffusivity of the HTPB-IPDI system, where diffusivity increased as a function of viscosity [31]. The

thermodynamic parameters were calculated using the Arrhenius and Eyring equations (Equations (7) and (8)) and are summarized in Table 2. The activation energy (E_{a1} and E_{a2}) were calculated from slope of plot log(k) versus (1/T) based on Equation (7) (Arrhenius equation) and was shown in Figure 5. The collision frequency factor (A) was calculated as intercept of plot ln(k) versus (1/T). Similarly, the relation of D versus (1/T) was plotted in Figure 5. The calculated activation energy of the noncatalytic part (Ea_1) and autocatalytic part (Ea_2) were 33.4 and 22.2 kJ/mol, respectively. The relationship between diffusion and temperature is described by the equation D = 3664.5/T − 10.034. The relations of reaction rate constant to temperature were k_1 = 1.9 + E11exp(−33.4/RT) and k_2 = 3.6 + E7exp (−22.2/RT).

Table 2. The thermodynamic parameter of HTPB-TDI system.

Part	E_a (kJ·mol^{-1})	Ln (A) (L·mol^{-1}·min^{-1})	ΔH (kJ·mol^{-1})	ΔS (kJ·mol^{-1}·K^{-1})
Noncatalytic (k_1)	33.4	1.9 + E11	3.6	−84.1
Autocatalytic (k_2)	22.2	3.6 + E7	2.3	−12.8

The activation enthalpy and entropy of curing were obtained from plotting ln(k/T) versus (1/T) following Equation (8) (Eyring equation), as shown in Figure 6. The value of (-ΔH) is the slope and (ΔS/R + ln(R/Nh) is the intercept. The values of ΔS and ΔH are also summarized in Table 2. It was observed that the activation entropy of k_1 was negatively larger than k_2, indicating that the catalytic part exhibited easier formation of the transition state.

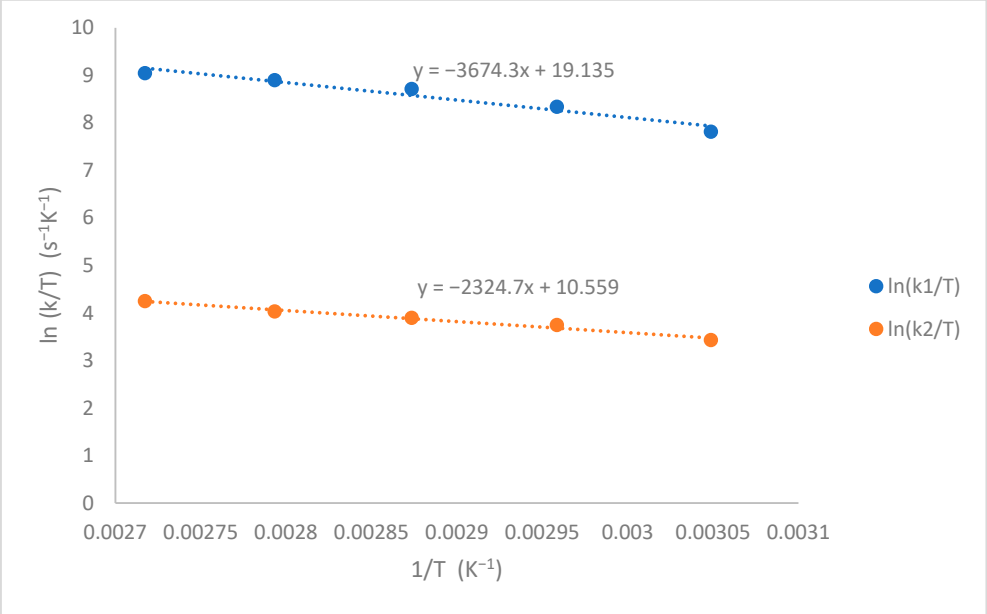


Figure 6. Plotting ln(k_1/T) and ln(k_2/T) versus (1/T) HTPB−TDI system.

Based on the calculated kinetic thermodynamic parameter, the reaction rate equation of HTPB-TDI is modeled by Equation (11).

$$\frac{d\propto}{dt} = \left[\left[1.9\times10^{11}exp\left(-\frac{33400}{RT}\right)(1-\propto)^{1.2}\right]\right] + \frac{\left[\left[3.6\times10^{7}exp\left(-\frac{22000}{RT}\right)\propto^{0.8}(1-\propto)^{1.2}\right]\right]}{[1+(\propto/(-10.034+3664/T))]} \quad (11)$$

3.4. Diisocyanate Effect

The plot of curing conversion polyurethane with HTPB-isocyanates at 30 °C is shown in Figure 7. Based on the curve, the overall reaction rate of polyurethane based HTPB is increased according to the isocyanate sequence used: TDI > IPDI > HMDI.

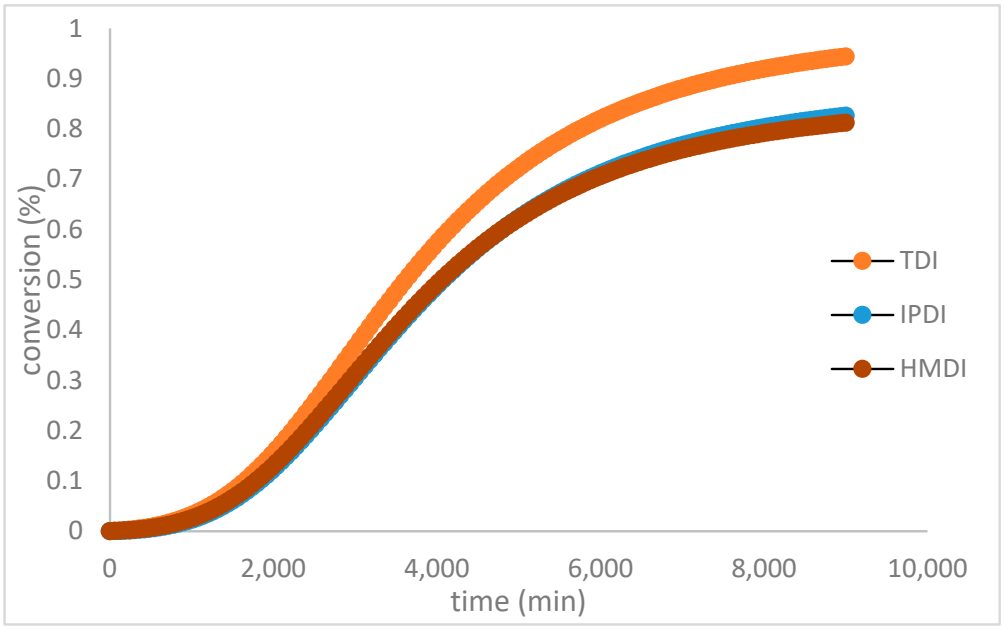


Figure 7. The curing conversion profile of polyurethane-based HTPB with various diisocyanates.

The kinetic parameters of polyurethane-based HTPB with various diisocyanates were evaluated and are summarized in Table 3. The effect of diisocyanate type on the reaction rate was evident from their respective activation energies. The reactivity of the noncatalytic rate constant (k_1) followed the order IPDI> TDI > HMDI, with activation energies of 33.4, 39.6, and 29.2 kJ·mol^{-1}, respectively. The autocatalytic rate constant (k_2) increased followed the order TDI > HMDI > IPDI with activation energy 22.2, 20.2, and 17.2 kJ·mol^{-1}. Both the noncatalytic and autocatalytic parts showed a similar trend in this regard. For the HTPB-IPDI system, the values of E_{a1} and E_{a2} were comparable to those of the autocatalytic model, with values of 45.12 and 54.12 kJ·mol^{-1} [30], as seen in Figure 8. The faster reactivity of HMDI compared to TDI can be attributed to their structural differences. The aliphatic nature of MDI resulted in less electron shifting towards the isocyanate group compared to the aromatic system of TDI, leading to a more negatively charged isocyanate, as observed in Figure 9. A similar reactivity pattern had been observed in experiments involving saturated polyester with HMDI and phenyl diisocyanate [32]. The reactivity of isocyanates was influenced by the positive nature of the carbon atom, which acted as a nucleophilic center.

Table 3. The kinetic parameters of polyurethane-based HTPB with various isocyanates.

System	E_{a1} (kJ·mol^{-1})	E_{a2} (kJ·mol^{-1})	D = A + B/T
HTPB-TDI	33.4	22.2	D = 3664/T − 10.03
HTPB-IPDI	39.6	17.2	D = 5489/T − 15.05
HTPB-HMDI	29.2	20.2	D = 4289/T − 11.74

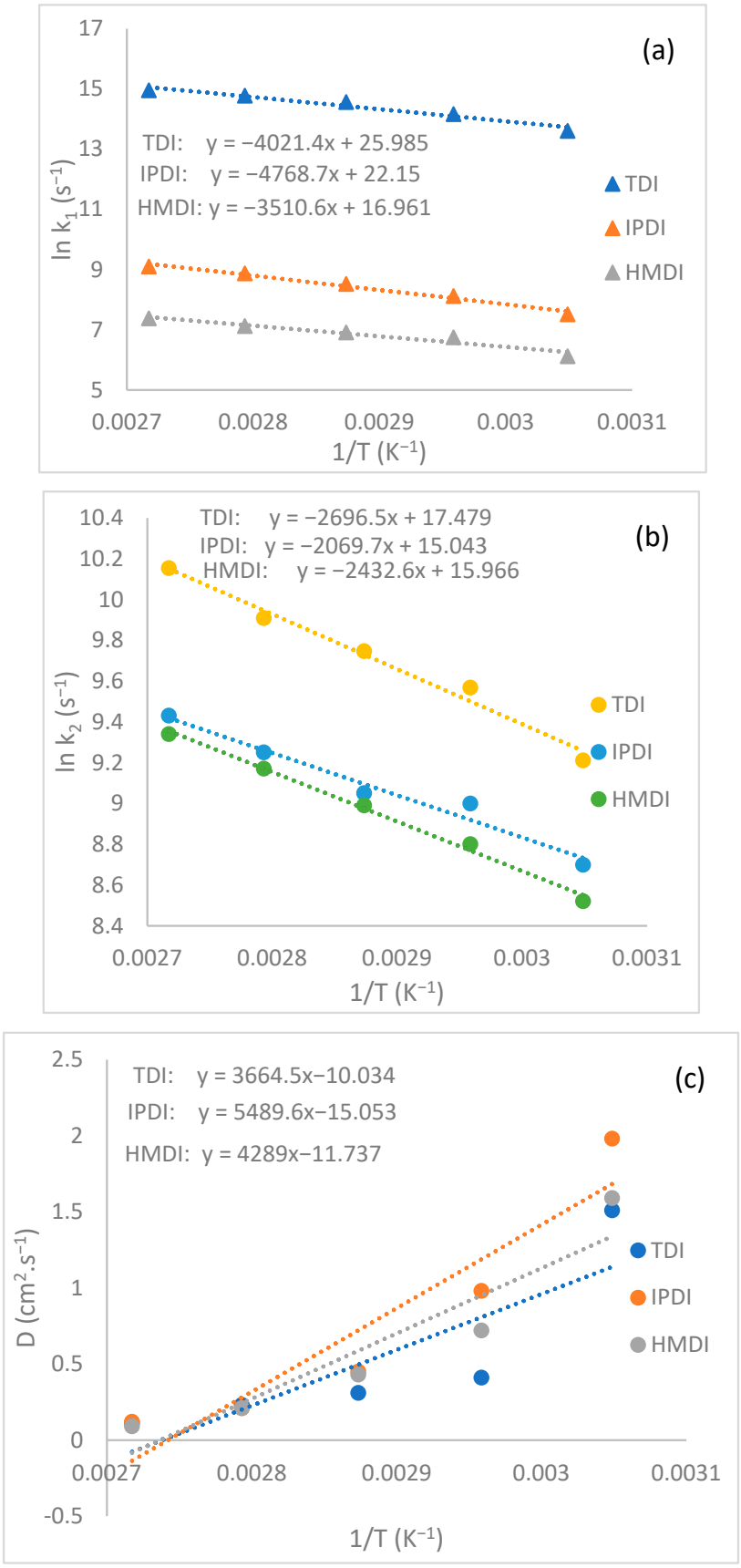


Figure 8. Plotting ln(k_1) vs. 1/T (**a**), ln (k_2) vs. 1/T (**b**), and D vs. (1/T) (**c**) with various isocyanates.

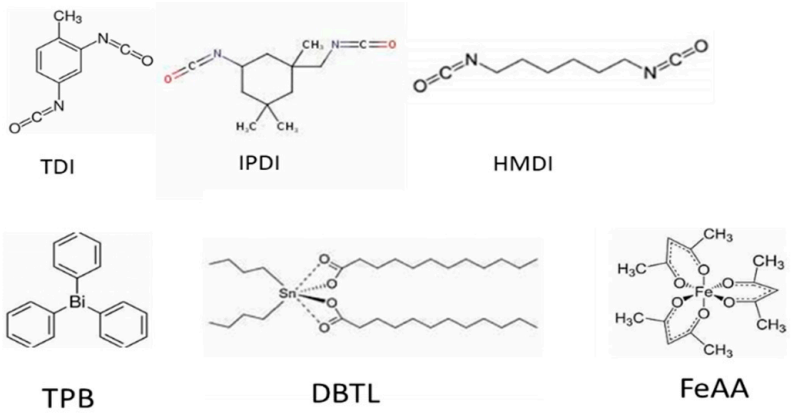


Figure 9. Structure of diisocyanate and catalyst.

The effect of diffusivity on the reaction rate is observed in Table 4. The effect of temperature to diffusivity is related to D = A + B/T, where A and B were intercept and slope of plot D to 1/T. The calculated slope value for the HTPB-IPDI system is similar to that observed in a previous experiment with a high filled state [31]. The diffusion effect was most significant in the following order: HTPB-HMDI > HTPB-TDI > HTPB-IPDI based on the slope values. It was important to note that the diffusion effect differs from the effect on the reaction rate and was primarily influenced by the movement of molecules. This diffusivity is directly related to the solubility of the substances, and the solubility could be predicted using group contribution methods based on the number of constituent groups in its molecular structure [31]. The calculated solubility values for HTPB, TDI, IPDI, and HMDI are 17.6, 13.8, 12.01, and 16.51 g·cm^{-3}, respectively. Among these, HTPB-HMDI had the lowest solubility, followed by HTPB-TDI and HTPB-IPDI. The diffusivity was directly related to the solubility of the substances, and the solubility could be predicted using group contribution methods of IPDI and TDI.

Table 4. Calculated solubility index of diisocyanate.

System	Calculated Solubility (g·cm^{-3})
HTPB	17.60
TDI	13.80
IPDI	12.01
HMDI	16.51
TPB	18.12
FeAA	15.35
DBTL	20.38
Ethyl acetate	20.80

3.5. Catalyst Addition

The effect of catalysts on the HTPB-TDI system was studied using TPB, FeAA, and DBTL. TPB and DBTL were commonly used as curing catalysts for composite propellants based on HTPB. The curing conversion profiles of HTPB-TDI with various catalysts are illustrated in Figure 10. All the added catalysts resulted in a higher slope compared to the system without any catalyst.

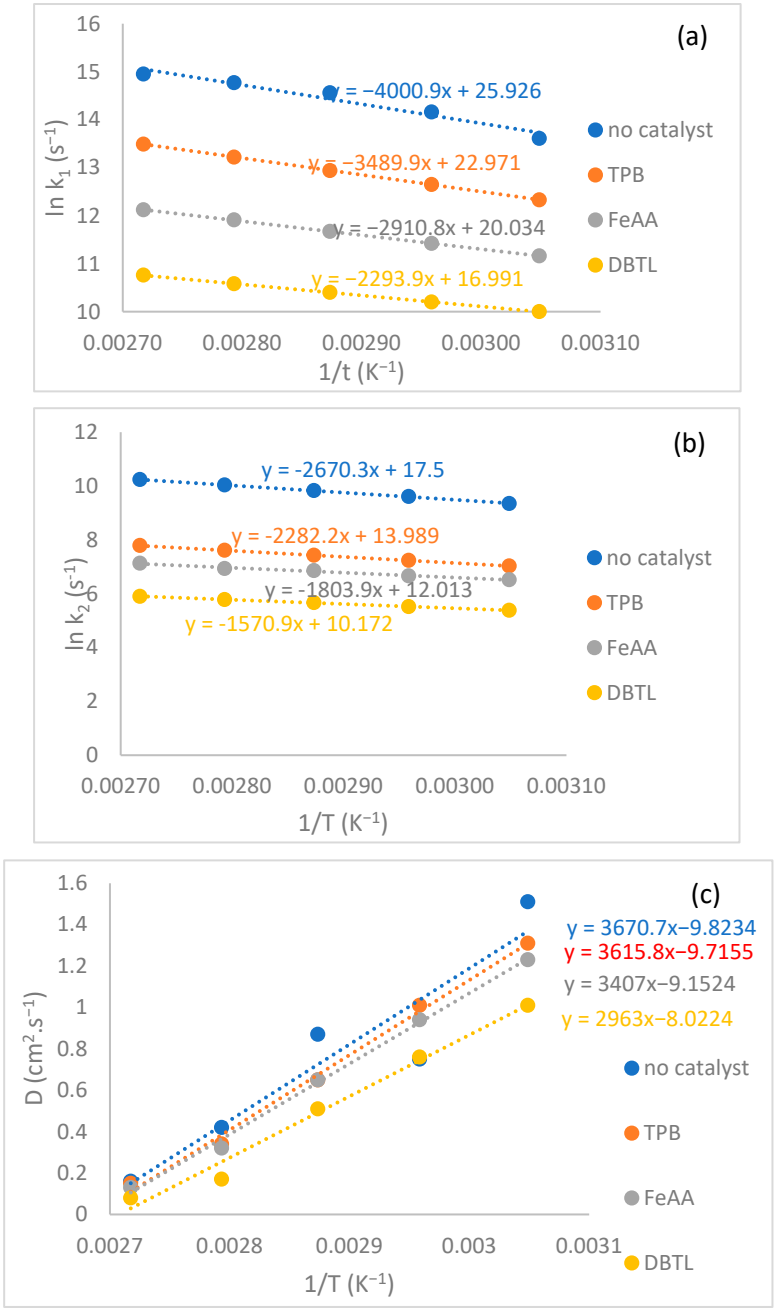


Figure 10. Plotting ln k_1 to (1/T) (**a**), ln k_2 to (1/T) (**b**) and (**c**) D to 1/T with various di-isocyanates.

The effect of adding catalysts on the activation energy and diffusivity of the curing process is summarized in Table 5. The activation energy decreases with the addition of catalysts: from 33.4 to 29.1 kJ·mol^{-1} for TPB, 24.1 kJ·mol^{-1} for FeAA, and 19.1 kJ·mol^{-1} for DBTL. The effectiveness of the catalysts in enhancing the reaction rate followed the order DBTL > TPB > FeAA. These results were consistent with previous experiments involving the addition of DBTL catalyst to HTPB-IPDI using the noncatalytic model. In those experiments, DBTL was found to decrease the activation energy from 41 to 38 kJ·mol^{-1}, 28 to 17 kJ·mol^{-1} for stearate-terminated hyperbranched polyether, and 35 to 31 kJ·mol^{-1} for TECH [21,33–35]. The addition of DBTL and TECH catalysts also decreased the gel time from 200 min to 16 min and 114 min, respectively [21]. The diffusivity also decreased with the addition of catalysts, following the same trend as the activation energy: DBTL > TPB > FeAA > TECH. This suggests that both reactivity and diffusivity were affected similarly by the addition of catalysts [17,22,24].

Table 5. The kinetic parameters of HTPB-TDI system with various catalysts.

System	E_{a1} (kJ·mol^{-1})	E_{a2} (kJ·mol^{-1})	D = A + B/T
HTPB-TDI no catalyst	33.4	22.2	D = 3670/T − 9.82
HTPB-TDI-TPB	29.1	19.0	D = 3616/T − 9.72
HTPB-TDI-FeAA	24.1	15.0	D = 3407/T − 9.15
HTPB-TDI-DBTL	19.1	13.0	D = 2963/T − 8.02

The phenomenon could be explained by the relationship between reactivity and the solubility of each catalyst [17,22,24]. Catalysts were added to accelerate the urethane formation, and polar interactions between hydroxyl or isocyanate and the catalyst occur, enhancing the electrophilic character of the carbon of the NCO groups [36]. Organotin catalysts, such as DBTL, followed a Lewis acid mechanism, as illustrated in Figure 3. Tin carboxylate bonds were hydroxylated to produce active intermediates, which then underwent nucleophilic attack by alcohol and the original C=O to form a Sn complexation. Isocyanate was activated by coordination to the active Sn-OR intermediate via oxygen or nitrogen, followed by the nucleophilic attack of the hydroxyl group from the alcohol.

The structure of the catalyst is illustrated in Figure 7, and it could be simplified into core and shell parts, with the core being rich in OH groups that were ready to form hydrogen bonds with NCO groups. The solubility parameters of TDI and HTPB were 13.8 and 17.6 g·cm^{-3}, respectively, while the solubility parameters of TPB, FeAA, DBTL, and ethyl acetate were 18.12, 15.35, 20.38, and 20.8 g·cm^{-3}. The higher solubility of the catalysts contributed to their OH-rich character, which enhanced their bonding with isocyanate. Higher solubility also increased their diffusivity.

4. Conclusions

Infrared spectroscopy was used to conduct a kinetic analysis of octogen coating with a polyurethane base containing hydroxyl-terminated polybutadiene (HTPB). The coating process involved a solvent method where octogen and liquid polyurethane were mixed, followed by solvent evaporation and curing at an elevated temperature. The curing process initially occurred in the solvent system and continued in the bulk system.

Kinetic analysis was performed using a modified diffusion–autocatalytic model, which includes noncatalytic, autocatalytic, and diffusion components. This model was effective in correcting errors observed in other models, particularly in the gel time region. The reaction rate was primarily controlled by chemical reactivity initially, but after the gel time, diffusion played a significant role. The diffusivity was influenced by temperature variations.

The reaction rate of di-isocyanates followed the sequence HMDI > TDI > IPDI due to their chemical structure. However, the effect of diffusivity increased in the sequence IPDI > HMDI > TDI, influenced by their solubility. When catalysts were added to the HTPB-TDI system, they significantly contributed to reducing the activation energy. The catalysts TPB, FeAA, and DBTL decreased the activation energy in the order DBTL > FeAA > TPB.

Author Contributions: Conceptualization, H.B.W. and H.R.D.S.; Data curation, H.B.W., H.R.D.S., A.J.F., D.S., A.F.Y. and M.B.; Formal analysis, H.B.W. and H.R.D.S.; Funding acquisition, H.B.W.; Investigation, H.B.W., H.R.D.S., Y.B., W.U.D., Y.A.I., R.A. and L.H.A.; Methodology, H.B.W., H.R.D.S. and K.H.; Project administration, H.B.W. and A.M.; Resources, H.B.W.; Software, H.B.W., H.R.D.S., A.J.F., A.R. and H.P.; Supervision, H.B.W.; Validation, H.B.W., H.R.D.S., B.W. and S.S.; Visualization, H.B.W.; Writing—original draft, H.B.W.; Writing—review and editing, H.B.W., H.R.D.S., S.S. and L.M. All authors have read and agreed to the published version of the manuscript.

Funding: The Authors would like to express their gratitude to Rispro-LPDP Fund Program Batch-II, through Competitive Research RISPRO-LPDP Program for financial support in doing this research with contract No. 082.01.06.3534.001.002.053A.524119 and Skep-27/LPDP/2020.

Institutional Review Board Statement: Not applicable.

Informed Consent Statement: Not applicable.

Data Availability Statement: The data presented in this study are available on request from the corresponding author.

Acknowledgments: The authors would like to convey our gratitude towards Rocket Technology Center and Dahana Co., Ltd.

Conflicts of Interest: The authors declare no conflict of interest.

References

1. Yano, Y.; Gomi, T. Burning Rate Characteristics of RDX-CMDB Propellants. *J. Jpn. Soc. Aeronaut. Space Sci.* **1986**, *34*, 447–452. [CrossRef]
2. Wang, Z.; Xue, Z.-H.; Meng, K.-J.; Zhang, X.-X.; Yan, Q.-L. Decomposition and Combustion of HTPB-Based Composite Propellants Containing Intercalated HMX Crystals with Desired High Energy but Low Burn Rate. *Fuel* **2022**, *321*, 124067. [CrossRef]
3. Wibowo, H.B. Current Solid Propellant Research and Development in Indonesia and Its Future Direction. *J. Phys. Conf. Ser.* **2018**, *1130*. [CrossRef]
4. Wu, Z.; Liu, N.; Zheng, W.; Chen, J.; Song, X.; Wang, J.; Cui, C.; Zhang, D.; Zhao, F. Application and Properties of CL-20/HMX Cocrystal in Composite Modified Double Base Propellants. *Propellants Explos. Pyrotech.* **2020**, *45*, 92–100. [CrossRef]
5. An, C.; Wang, J.; Xu, W.; Li, F. Preparation and Properties of HMX Coated with a Composite of TNT/Energetic Material. *Propellants Explos. Pyrotech.* **2010**, *35*, 365–372. [CrossRef]
6. Wei An, C.; Li, F.-S.; Song, X.-L.; Wang, Y.; Guo, X.-D. Surface Coating of RDX with a Composite of TNT and an Energetic-Polymer and Its Safety Investigation. *Propellants Explos. Pyrotech.* **2009**, *34*, 400–405. [CrossRef]
7. Wibowo, H.B.; Dharmawan, W.C.; Wibowo, R.S.M. Bulk Polymerization Kinetics of Hydroxy Terminated Polybutadiene and Toluene Diisocyanate with Infrared Spectroscopy. *Indones. J. Chem.* **2018**, *18*, 552. [CrossRef]
8. Wibowo, H.; Sitompul, H.; Budi, R.; Hartaya, K.; Abdillah, L.; Ardianingsih, R.; Wibowo, R. Hexogen Coating Kinetics with Polyurethane-Based Hydroxyl-Terminated Polybutadiene (HTPB) Using Infrared Spectroscopy. *Polymers* **2022**, *14*, 1184. [CrossRef]
9. Lee, S.; Hong, I.-K.; Lee, J.W.; Jeong, W.B. Rheology and Curing of Hydroxyl Terminated Polybutadiene/(Sugar or Calcium Carbonate) Suspension. *Polym. Korea* **2014**, *38*, 417–424. [CrossRef]
10. Neudorfl, P.S.; Back, R.A.; Douglas, A.E. The Absorption Spectrum of Trans-Diimide (N2H2) in the Vacuum Ultraviolet Region1. *Can. J. Chem.* **1981**, *59*, 506–517. [CrossRef]
11. Bondybey, V.E.; Nibler, J.W. Infrared and Raman Spectra of Solid and Matrix Isolated Diimide, HNNH. *J. Chem. Phys.* **1973**, *58*, 2125–2134. [CrossRef]
12. Joshi, N.; Romanias, M.N.; Riffault, V.; Thevenet, F. Investigating Water Adsorption onto Natural Mineral Dust Particles: Linking DRIFTS Experiments and BET Theory. *Aeolian Res.* **2017**, *27*, 35–45. [CrossRef]
13. da Costa Mattos, E.; Moreira, E.D.; Diniz, M.F.; Dutra, R.C.L.; da Silva, G.; Iha, K.; Teipel, U. Characterization of Polymer-Coated RDX and HMX Particles. *Propellants Explos. Pyrotech.* **2008**, *33*, 44–50. [CrossRef]
14. Wibowo, H.B.; Wibowo, R.S.M. Non Energetic Binder Application for RDBP Propellant Based Large Caliber Munition (MKB). In Proceedings of the International Seminar on Aerospace Science and Technology (ISAST), Lombok, Indonesia, 20–22 September 2016; pp. 82–91.
15. Wibowo, H.B. Isomerisasi Polimer Melalui Reaksi Sain Sayef Untuk Mengubah Konfigurasi HTPB (Hydroxyl Terminated Polybutadiene) Polymer Isomerization by Sain Sayef Reaction to Modify Configuration of HTPB (Hydroxyl Terminated Polybutadiene). *J. Teknol. Dirgant.* **2016**, *14*, 137–146. [CrossRef]
16. Gopala Krishnan, P.S.; Ayyaswamy, K.; Nayak, S.K. Hydroxy Terminated Polybutadiene: Chemical Modifications and Applications. *J. Macromol. Sci. Part A* **2013**, *50*, 128–138. [CrossRef]
17. Navarchian, A.H.; Picchioni, F.; Janssen, L.P.B.M. Rheokinetics and Effect of Shear Rate on the Kinetics of Linear Polyurethane Formation. *Polym. Eng. Sci* **2005**, *45*, 279–287. [CrossRef]
18. Betoret, E.; Betoret, N.; Carbonell, J.V.; Fito, P. Effects of Pressure Homogenization on Particle Size and the Functional Properties of Citrus Juices. *J. Food Eng.* **2009**, *92*, 18–23. [CrossRef]
19. Argade, P.S.; Magar, D.D.; Saudagar, R.B. Solid Dispersion: Solubility Enhancement Technique for Poorly Water Soluble Drugs. *J. Adv. Pharm. Educ. Res.* **2013**, *3*, 427–439.
20. Tow, G.M.; Maginn, E.J. Cross-Linking Methodology for Fully Atomistic Models of Hydroxyl-Terminated Polybutadiene and Determination of Mechanical Properties. *Macromolecules* **2021**, *54*, 4488–4496. [CrossRef]
21. Du, W.; Tan, L.; Zhang, Y.; Yang, H.; Chen, H. Rheological and Kinetic Investigation into Isothermal Curing of a Thermoset Polythiourethane System. *Polym.-Plast. Technol. Mater.* **2020**, *59*, 63–71. [CrossRef]
22. Guo, J.; Chai, T.; Liu, Y.; Cui, J.; Ma, H.; Jing, S.; Zhong, L.; Qin, S.; Wang, G.; Ren, X. Kinetic Research on the Curing Reaction of Hydroxyl-Terminated Polybutadiene Based Polyurethane Binder System via FT-IR Measurements. *Coatings* **2018**, *8*, 175. [CrossRef]

23. Bardestani, R.; Patience, G.S.; Kaliaguine, S. Experimental Methods in Chemical Engineering: Specific Surface Area and Pore Size Distribution Measurements—BET, BJH, and DFT. *Can. J. Chem. Eng.* **2019**, *97*, 2781–2791. [CrossRef]
24. Song, X.; Yunjun, L. Effect of Hyperbranched Polyesters on HTPB Polyurethane Curing Kinetic. *Mater. Res.* **2013**, *17*, 78–82. [CrossRef]
25. Sun, Z.; Xi, G.; Chen, X. A Numerical Study of Stir Mixing of Liquids with Particle Method. *Chem. Eng. Sci.* **2009**, *64*, 341–350. [CrossRef]
26. Verhoeven, V.W.A.; Padsalgikar, A.D.; Ganzeveld, K.J.; Janssen, L.P.B.M. A Kinetic Investigation of Polyurethane Polymerization for Reactive Extrusion Purposes. *J. Appl. Polym. Sci.* **2006**, *101*, 370–382. [CrossRef]
27. Tanver, A.; Huang, M.H.; Luo, Y.J.; Hei, Z.H. Chemical Kinetic Studies on Polyurethane Formation of GAP and HTPB with IPDI by Using In Situ FT-IR Spectroscopy. *Adv. Mat. Res.* **2014**, *1061–1062*, 337–341. [CrossRef]
28. Sun, L.; Zong, Z.; Xue, W.; Zeng, Z. Mechanism and Kinetics of Moisture-Curing Process of Reactive Hot Melt Polyurethane Adhesive. *Chem. Eng. J. Adv.* **2020**, *4*, 100051. [CrossRef]
29. Toosi, F.S.; Shahidzadeh, M.; Ramezanzadeh, B. An Investigation of the Effects of Pre-Polymer Functionality on the Curing Behavior and Mechanical Properties of HTPB-Based Polyurethane. *J. Ind. Eng. Chem.* **2015**, *24*, 166–173. [CrossRef]
30. Lucio, B.; de la Fuente, J.L. Kinetic and Thermodynamic Analysis of the Polymerization of Polyurethanes by a Rheological Method. *Thermochim. Acta* **2016**, *625*, 28–35. [CrossRef]
31. Santhosh, G.; Reshmi, S.; Reghunadhan Nair, C.P. Rheokinetic Characterization of Polyurethane Formation in a Highly Filled Composite Solid Propellant. *J. Therm. Anal. Calorim.* **2020**, *140*, 213–223. [CrossRef]
32. Ou, Y.; Sun, Y.; Jiao, Q. Properties Related to Linear and Branched Network Structure of Hydroxyl Terminated Polybutadiene. *e-Polymers* **2018**, *18*, 267–274. [CrossRef]
33. Lee, S.; Choi, C.H.; Hong, I.-K.; Lee, J.W. Polyurethane Curing Kinetics for Polymer Bonded Explosives: HTPB/IPDI Binder. *Korean J. Chem. Eng.* **2015**, *32*, 1701–1706. [CrossRef]
34. Lee, S.; Choi, J.H.; Hong, I.-K.; Lee, J.W. Curing Behavior of Polyurethane as a Binder for Polymer-Bonded Explosives. *J. Ind. Eng. Chem.* **2015**, *21*, 980–985. [CrossRef]
35. Song, X.; Luo, Y. Curing Kinetics Study on Interpenetrating Polymer Networks Based on Modified Hyperbranched Polyether/Polyurethane. *Monatshefte Chem.-Chem. Mon.* **2017**, *148*, 1323–1328. [CrossRef]
36. Hui, M.; Liu, Y.-C.; Chai, T.; Hu, T.-P.; Guo, J.-H.; Yu, Y.-W.; Yuan, J.-M.; Wang, J.-H.; Qin, N.; Zhang, L. Kinetic Studies on the Cure Reaction of Hydroxyl-Terminated Polybutadiene Based Polyurethane with Variable Catalysts by Differential Scanning Calorimetry. *e-Polymers* **2017**, *17*, 89–94. [CrossRef]

Disclaimer/Publisher's Note: The statements, opinions and data contained in all publications are solely those of the individual author(s) and contributor(s) and not of MDPI and/or the editor(s). MDPI and/or the editor(s) disclaim responsibility for any injury to people or property resulting from any ideas, methods, instructions or products referred to in the content.